Thermochimica Acta, 197 (1992) 307–318
Elsevier Science Publishers B.V., Amsterdam

Effect of thermal treatment on the kinetics and sintering characteristics of nickel hydroxide as a precursor for the thermal genesis of nickel oxide catalyst

R.M. Gabr, A.N. El-Naimi [1] and M.G. Al-Thani [1]

Chemistry Department, Faculty of Science, Assiut University, Assiut (Egypt)

(Received 19 July 1991)

Abstract

The thermal events encountered throughout the calcination course of the parent nickel hydroxide precursor were investigated using a number of physicochemical techniques. The thermal decomposition products obtained by calcination of this precursor were investigated by infrared and X-ray techniques. Analysis of the surface excess oxygen and N_2 adsorption data revealed the existence of a considerable disparity in their degrees of oxidation, surface area and pore structure. The variation of the surface area with time was correlated with the differences in the concentration of the created cationic vacancies during the calcination. The presence of such vacancies leads to an increase in the growth rate of the fine pores compared with the large ones. A reduction in the volume of the pores which are intercommunicating and which communicate with the surface of the catalyst, was observed at a certain moment during the sintering process of the products obtained. The thermal decomposition of the parent hydroxide was studied non-isothermally and isothermally. The kinetic analysis of the $\alpha-t$ data obtained under isothermal conditions in the temperature range 250–350°C was performed. From the complementary consideration of the sintering study and the kinetic evidence we can conclude that the thermal decomposition of the hydroxide occurs by a nucleation-and-growth reaction and that the main decomposition process obeys the Avrami–Erofe'ev equation. During the decomposition course, the nucleation reaction is followed by an advancing interface mechanism in the brucite-type structure of the reactant, and both proton and electron transfer steps are involved.

INTRODUCTION

It has been stated [1] that during the thermal treatment of crystalline hydroxides, the mechanism which determines the relationship between the surface and the calcination temperature is governed by three consecutive processes: decomposition, recrystallization and sintering. Release of water from the crystalline hydroxide (decomposition or dehydroxylation) differs

Correspondence to: R.M. Gabr, Chemistry Department, Faculty of Science, Assiut University, Assiut, Egypt.
[1] Present address: Chemistry Department, Qatar University, Doha, Qatar.

from the dehydration of the crystalline hydrate in that product release must be preceded by chemical interaction between the anions; the role of proton transfer in such a process has been discussed [2,3]. The effect of calcination on the residual oxide products has been studied by gas adsorption measurements [4,5]. Creep and sintering of the product phase have been observed [6,7]. Water elimination is regarded as the first step in a sequence of structurally related steps through which the hydroxide is converted to the thermally stable oxide; the water is produced by the interaction of the double hydroxide layers and escapes through these layers by diffusion [8]. It has been proposed [9] that sintering of crystalline solids occurs on account of their "viscous flow", and may be related to directional displacement of vacancies. It is interesting to consider the existence of directional movement of atoms during sintering of crystallites, leading to filling of their pores and grain growth. It has been stated [10] that the equilibrium vacancy concentration cannot be uniform at different points in the porous solid, or in a body having internal surfaces, or in a solid homogeneous body of irregular form, the surface of which does not correspond to the minimum free energy.

The present work deals with a study of the nature and characteristics of both sintering and decomposition processes accompanying the thermal treatment of nickel hydroxide. Structural and textural variations encountered throughout the calcination course were followed by TGA, DTA, X-ray diffraction, IR analysis and adsorption measurements of N_2 gas.

EXPERIMENTAL

Materials

Nickel hydroxide was prepared [11] by treating nickel nitrate (AR-grade, Merck product) solution with an excess of ammonium hydroxide, followed by steam distillation until the precipitate was ammonia free. After drying over P_2O_5, the dried product had a water content of 20.09%, compared with 19.43% for the stoichiometric $Ni(OH)_2$.

The N_2 gas used has a nominal purity of 99.7%. It was further purified by passing it through an appropriate series of oxisorb and molecular sieve traps.

Apparatus and techniques

Thermogravimetric (TG) and differential thermal (DTA) analyses of the parent hydroxide were carried out using a Shimadzu unit (Model 30H). The heating rate was standarized at 10°C min^{-1} in a dynamic atmosphere of air (15 ml min^{-1}); highly sintered α-Al_2O_3 was used as a thermally inert reference for the DTA measurements.

Infrared absorption spectra (IR) were recorded from thin discs (40 ± 2 mg cm^{-1}) of KBr-supported test samples over the frequency range 4000–200 cm^{-1}, using a Perkin–Elmer spectrophotometer (Model 2000).

X-ray powder diffractograms (XRD) were recorded for the calcinated products of the parent hydroxide on a Philips diffractometer (Model PW 1710), using Ni-filtered Cu Kα radiation, operated with 20° diverging and receiving slits at a scanning rate of 20° min^{-1}. The diffraction patterns thus obtained were matched with relevant ASTM cards [12] for identification purposes.

The surface excess charge associated with the nickel ions was determined by allowing the excess oxygen to decompose hydrazine $N_2H_4 + O_2 \rightleftharpoons N_2 + 2H_2O$. The undecomposed N_2H_4 was evaluated automatically using the apparatus and technique described elsewhere [13].

Nitrogen sorption was determined volumetrically at 77 K using a conventional apparatus. The calcined samples were pre-outgassed (10^{-5} torr) at 150°C for 5h. The surface area (S_{BET}) was calculated using the BET method. Analysis based on the Kelvin equation was performed for calculating the pore-size distribution data.

RESULTS AND DISCUSSION

The non-isothermal events encountered throughout the calcination course of the parent hydroxide are shown in the TG and DTA curves in Fig. 1. The TG curve (a) indicates that the hydroxide suffers a 20.90% weight loss through a single acceleratory-rate step occurring at 275–325°C which is compatible with that anticipated theoretically (19.43%) for the formation of the stoichiometric NiO structure. The endothermic peak observed in the DTA curve (b) at about 310°C, and its compatibility with the region of the weight loss in the TG curve, supports the idea that the decomposition reaction proceeds through a single distinct stage.

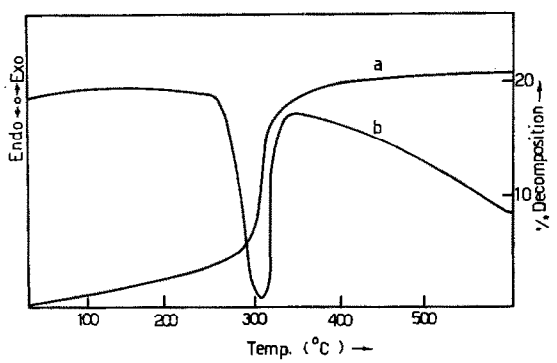

Fig. 1. TG (a) and DTA (b) curves for nickel hydroxide.

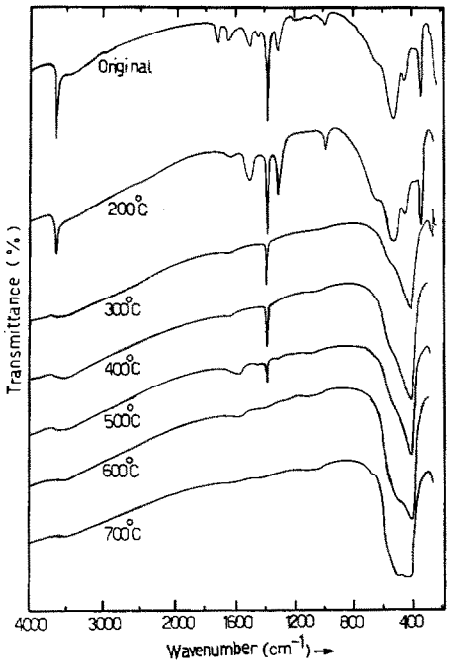

Fig. 2. Infrared absorption spectra of the parent nickel hydroxide and its calcination products at 200, 300, 400, 500, 600 and 700°C.

Structural variations accompanying the thermal treatment of the parent hydroxide were investigated from the IR spectra (Fig. 2) and XRD data (Fig. 3), as well as from the surface content of excess oxygen determined for the calcined product of the parent hydroxide (Table 1). The IR spectra for the parent sample and its calcination product at 200°C show characteristic bands [14] for structural (OH^-) (3650 cm^{-1}) and water of hydration (370 cm^{-1}) [15]. Because the adsorbed oxygen species are known [16] to absorb IR radiation at 1552 cm^{-1} (O_2), at about 1160 cm^{-1} (O_2^-) and at about 860 cm^{-1} (O_2^{2-}); the complex absorption band observed at 1500–980 cm^{-1} can be assigned to the presence of a mixture of perturbed O_2^- and O_2^{2-} species. For the calcination products obtained at 300–500°C, the IR spectra show characteristic peaks of charged as well as uncharged O_2 species [17]. Within this context, the XRD data compiled in Fig. 3 indicate the coexistence of Ni_2O_3 with the dominant NiO phase; this is reflected in the relevant IR spectra of these products, which show marked changes in comparison with the band structure of the parent hydroxide. In addition, the maximum surface content of excess oxygen determined for this temperature range, see Table 1, confirms the above results. At 500°C, where the decomposition process is complete, a marked decrease in surface excess oxygen content is observed. This may help to clarify the interrelation already inferred from the XRD analysis, which confirmed the formation of

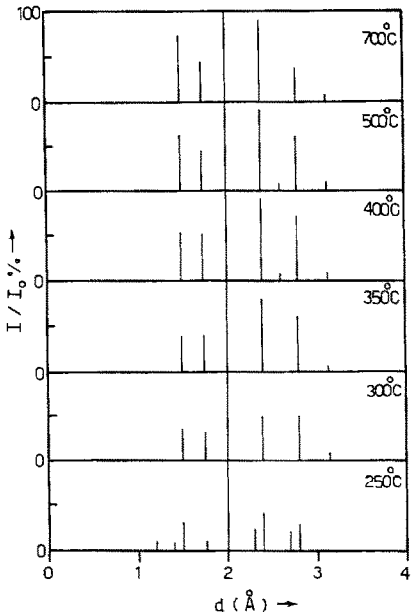

Fig. 3. XRD for nickel hydroxide and its calcination products at 250, 300, 350, 400, 500 and 700°C.

NiO as the sole bulk phase. The relevant IR spectrum shows a band characteristic for the uncharged O_2 species at about 1500 cm^{-1}. The IR spectra for the products obtained above 500°C show only the absorptions of Ni=O bending vibrations, where the spectra display a well defined band structure analogous to that reported for the NiO-like structure [11]. The corresponding XRD data for these products also support the above contention.

It is worth noting that at such high temperatures, the lattice ordering mechanism is operating and is accompanied by a sintering process [18]. Therefore, the unexpected slight increase in the determined surface content of excess oxygen (700°C), Table 1, is understandable if we remember that the sintering process tends to maintain the bulk properties throughout the solid particles [18].

Sintering is one of the most important phenomena taking place when crystalline solids are heated. It can affect both the decomposition reaction and also the properties of the resulting products. Moreover the external sign of sintering in a crystalline porous solid, specially a dispersed one, is a reduction in its external dimensions during heating. Therefore a reduction in porosity and an increase in the apparent density are observed with an increase in calcination temperature (see Table 1).

Sintering of a powder normally begins with the "welding" of the grains at the contact sites. This affects the trend of variation of the surface area with the duration time, as shown in Fig. 4. There is a decrease in S_{BET} at

TABLE 1

Sintering rate constants and cumulative data for the calcination products of nickel hydroxide

Calcination temperature (°C)	S_{BET} ($m^2\ g^{-1}$)	Density ($g\ cm^{-3}$)	V_p ($ml\ g^{-1}$)	$\bar{r}_p$ (Å)	S_{cum} ($m^2\ g^{-1}$)	Surface excess oxygen ($mg\ O_2\ g^{-1}$)	Sintering rate constant ($m^2\ g^{-1}$)
250	17.77	1.42	0.241	27	10.1	3.6	0.037
300	52.12	1.84	0.973	37	49.3	4.8	0.025
350	46.97	1.98	0.432	18	44.8	5.3	0.100
400	40.27	2.21	0.268	13	39.9	4.9	0.160
500	21.23	2.33	0.198	18	20.9	2.7	0.320
700	6.08	2.51	0.087	28	6.05	3.3	1.800

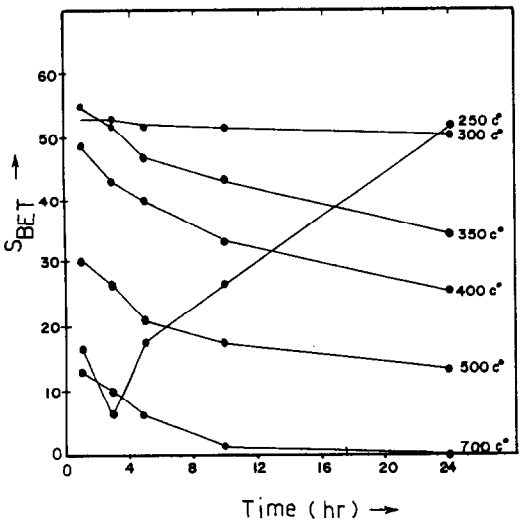

Fig. 4. Variation of surface area (S_{BET}) with time duration of heating at different calcination temperatures for nickel hydroxide.

temperatures above 300°C which can be interpreted as follows. Sintering can be represented as the spontaneous filling of the free spaces inside the grains and between them by substance as a result of an increase in the mobility of the elements in its lattice at adequately high temperatures. As a result, there is a regular change in the area of the entire surface of the grains and the surface of contact between them: the first diminishes and the second increases, leading to the observed surface area decrease. Therefore special attention was paid to the kinetics of sintering in a work dealing with the adsorption capacity of these solids [19,20].

Regarding the kinetic expression for the sintering rate on the basis [19] of surface area variation with the calcination temperature and duration time, the rate of an active solid is represented by

$$dS/dt = -Kf(S)t \tag{1}$$

where S_{BET} is denoted as S.

When an active solid is heated, S_{BET} can be correlated directly [19] with the rate of sintering according to the equation

$$dS/dt = -KS \tag{2}$$

which can be written in the form

$$S = S_0 \exp(-Kt) \tag{3}$$

Using eqn. (3), the sintering rate constants were calculated, see Fig. 5, and are listed in Table 1 together with the cumulative data derived from the analysis of N_2 adsorption measurements for the calcined products of nickel hydroxide at 250–700°C. From studying the trend of variation of the

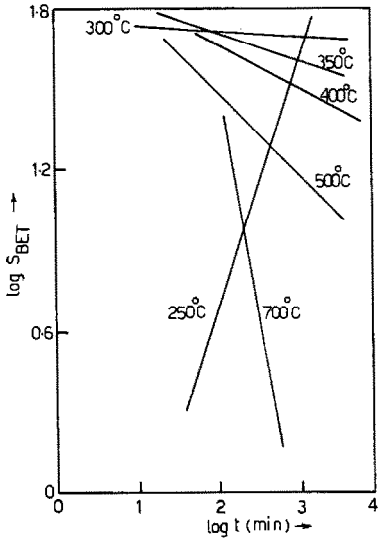

Fig. 5. Variation of log S_{BET} with log t for the calcination products of nickel hydroxide at different temperatures (250–700°C).

obtained kinetic data of sintering with time at constant temperature, represented in Fig. 5 and Table 1, we can conclude that the degree of shrinkage of the solid is proportional to the duration time. This is in accordance with the results given by Pines [10], who related this behaviour to the change in the coefficient of self diffusion as a result of a process of relaxation (removal of distortions), occurring simultaneously with sintering.

One of the main factors influencing the sintering rate is the crystallization and grain growth process which occur concurrently. It was found (Table 1) that the sintering rate is greatly reduced when there is intensive grain growth. This is explained by the fact that diffusion from the pores occurs not towards the surface of the particles but towards the boundaries of the individual grains [10]. Thus, the distance over which diffusion occurs with a reduction in pores is determined by the sizes of the crystals which sharply reduced during intensive accumulative recrystallization [21,22].

It has been stated previously [11] that the thermal treatment of nickel hydroxide produces an oxide containing excess oxygen in the lattice and chemisorbed on the surface. This excess oxygen is accompanied by the creation of cationic vacancies $|C|$, which facilitate surface as well as lattice diffusion [11] at higher temperatures

$$2Ni^{2+} + 2O^{2-} + \tfrac{1}{2}O_2(g) \rightleftharpoons 2Ni^{3+} + 3O^{2-} + |C| \qquad (4)$$

Accordingly the concentration of the surface excess oxygen can be considered as a measure of the concentration of these vacancies. In our case it was found that the surface excess oxygen increases with increasing calcination temperature (Table 1). It has been stated [9] that (i) the difference in

the concentration of the vacancies leads to an increase in the growth rate of the fine pores compared with the large ones, and (ii) the fine pores may diminish at the expense of an increase in the volume of the large ones. These conclusions are in agreement with the cumulative data cited in Table 1. Thus, if we assume that the calcination products contain closed pores of different sizes, their growth will be irregular and depends on many factors, acting partly in opposite directions and behaving differently for different pores at various stages of the sintering process. Accordingly, the process of reducing the volume of the pores which are intercommunicating and which communicate with the surface of the oxide system obviously occurs during the sintering process.

Extending the kinetic study of the sintering process, the activation energy value (E_a) for this process was calculated to be 17.14 kJ mol^{-1}. The lower value of E_a suggests that the decomposition reaction is the rate-determining step, which normally possesses higher E_a values [3]. Therefore any further attempt to justify the above conclusion must depend on the kinetics of the thermal analysis.

Next, the results of fundamental mechanistic investigations of the thermal decomposition of a well-defined solid will be discussed. Such studies are intended to identify the sequence of steps by which such a crystalline compound is converted to the reaction products, and also the parameters which control the reactivity of the participating species. Therefore the above analysis is of particular significance, because the conclusions that will be reached provide a theoretical basis for the meaningful interpretation of the previously obtained data.

The kinetics of thermal decomposition in both isothermal and non-isothermal conditions have interested several investigators [23–25]. Because of several inaccuracies [26,27], reliable kinetic parameters cannot be easily obtained from a single variable temperature thermogram [28]. Accordingly, isothermal kinetic analyses are in general more reliable for determining the α–t function and the E_a value of the reaction, especially under less complex conditions [29–31].

The α–t curves for the parent hydroxide were obtained in the temperature range 250–350°C. In order to carry out the scheme of kinetic analysis, a computer program was devised [32] considering the different rate equations [25] governing the kinetics of solid state reactions. It was found from the analysis of each set of α–t data that the main decomposition process of nickel hydroxide obeys the Avrami–Erofe'ev equation

$$-\log(1-\alpha)^{1/n} = Kt \tag{5}$$

Accordingly, the decomposition reaction occurs by a nucleation-and-growth mechanism. This nucleation occurs at all edges of the plate-like crystallites and the subsequent advance of the coherent interface represents a topotactic process [33] yielding a pseudomorphic product, within which the pores

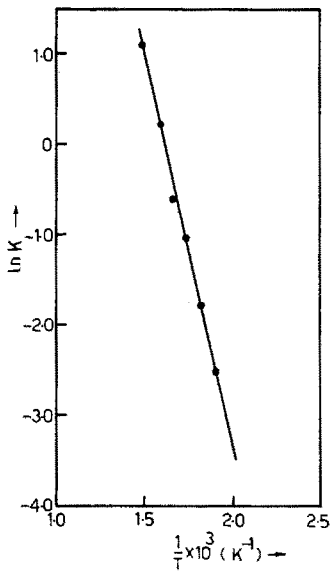

Fig. 6. Arrhenius plot for the isothermal decomposition of nickel hydroxide.

are disposed in a regular manner. The activation energy (E_a) for the decomposition reaction was estimated as 177.11 kJ mol^{-1} from the rate constants measured between 250 and 350°C by applying the Arrhenius equation, see Fig. 6. On the whole, the possible association of surface excess oxygen with O^{2-} and OH^-, stresses the validity of the concept [11] that NiOOH is formed as an intermediate and is confined to the surface layers. The formation of such species is a result of the following topochemical decomposition reaction

$$2Ni(OH)_2 + \tfrac{1}{2}O_2 \rightleftharpoons 2NiOOH + H_2O \qquad (6)$$

Thus, the formation of stoichiometric NiO can be attributed [34,35] to the presence of insufficient ambient oxygen to initiate such a topochemical process.

The above findings lead to the suggestion that the proposed nucleation-and-growth mechanism is followed by an advancing interface in the brucite-type structure of the reactant and both proton transfer ($2OH^- \rightarrow H_2O + O^{2-}$) and electron transfer ($2Ni^{3+} + O^{2-} \rightarrow 2Ni^{2+} + \frac{1}{2}O_2$) steps are involved. The higher value of E_a (177.11 kJ mol^{-1}) is ascribed to the participation of the electron transfer step at low temperatures, whereas at temperatures above 310°C (DTA), water escape becomes inhibited so that the dehydroxylation exerts the dominant influence on the decomposition rate. In a general consideration of the mechanisms whereby water may be eliminated from solids, we can conclude [36–38] that four steps may contribute to the overall decomposition reaction: (i) formation of the water molecule within the crystal, (ii) water elimination at the gas–solid interface,

(iii) fragmentation of the reactant crystal, and (iv) reorganization of the vacancy structure.

REFERENCES

1 R.B. Fahim and K.M. Abd El-Salaam, J. Catal., 9 (1967) 63.
2 N.H. Brett, K.J.D. Mackenzie and J.H. Sharp, Quart. Rev., 24 (1970) 185.
3 W. Gieseke, H. Naegerl and F. Freund, Naturwissenschaften, 57 (1970) 493.
4 M. Faure and B. Imelik, Bull. Soc. Chem. Fr., (1971) 761.
5 P.J. Anderson and R.F. Horlock, Trans. Faraday Soc., 65 (1969) 251.
6 R.M. Dell, Inst. Chem. Eng. Symp. Ser., 27 (1968) 3.
7 P.W. Sunderland and A.C.D. Chaklader, J. Am. Ceram. Soc., 52 (1969) 410.
8 J.F. Googman, Proc. R. Soc. London Ser. A., 247 (1958) 346.
9 Ya. I. Frenkel, Zh. Eksp. Teor. Fiz., 16 (1946) 39.
10 B.Ya. Pines, Usp. Fiz. Nauk, 62 (1954) 501.
11 M.I. Zaki, S.A.A. Mansour and R.B. Fahim, Surf. Technol., 25 (1985) 287.
12 W.F. McClune (Ed.), Powder Diffraction File (Inorganic Compounds), JCPDS, PA, 1978.
13 A. Bielanski and M. Najbar, J. Catal., 25 (1972) 398.
14 J.A. Gadsden, Infrared Spectra of Minerals and Related Inorganic Compounds, Butterworths, London, 1975.
15 F.A. Miller, G.L. Carlson, F.F. Bentley and W.H. Jones, Spectrochim. Acta., 16 (1960) 135.
16 N. Sheppard, in R.F. Willis (Ed.), Vibration Properties of Adsorbates, Springer-Verlag, Berlin, 1980.
17 F. Al-Mashta, N. Sheppard, V. Lorenzelli and G. Busca, J. Chem. Soc. Faraday Trans. 1, 78 (1982) 979.
18 F. Fievet and M. Figlarz, J. Catal., 39 (1975) 350.
19 K.M. Abd El-Salaam, R.M. Gabr and A.A. Said, Surface Technol., 9 (1979) 427.
20 S.J. Gregg and K.S.W. Sing, Adsorption Surface Area and Porosity, Academic Press, London, 1982.
21 J.E. Burke, J. Am. Ceram. Soc., 40 (1957) 80.
22 W.D. Kingery, Introduction to Ceramics, New York, 1960, section 122.
23 L.G. Harrison, C.H. Bamford and C.F.M. Tipper, Comprehensive Chemical Kinetics, Vol. 2, Elsevier, Amsterdam, 1969.
24 A.K. Galwey, D.M. Jamison, M.E. Brown and M.J. McGinn, Reaction Kinetics in Heterogeneous Chemical Systems, Elsevier, Amsterdam, 1975.
25 R.M. Gabr, A.M. El-Awad and M.M. Girgis, Thermochim. Acta, in press.
26 K. Akita and M. Kase, J. Phys. Chem., 72 (1968) 906.
27 R. Melling, F.W. Wilburn and R.M. McIntosh, Anal. Chem., 41 (1969) 1275.
28 G.C.T. Guarini, R. Spinicci, F.M. Carlini and D. Donati, J. Therm. Anal., 5 (1973) 307.
29 D. Broadbent, D. Dollimore and J. Dollimore, J. Chem. Soc. A, (1966) 1491.
30 T.B. Flanagan, J.W. Simons and P.M. Fichte, J. Chem. Soc. Chem. Commun., (1971) 370.
31 A.K. Galwey, M.J. McGinn and M.E. Brown, in, J.S. Anderson, M.W. Roberts and F.S. Stone (Eds.), Reactiv. Solids, Proc. 7th Int. Symp., London, 1972, p. 431.
32 The program listing and subroutines are available on request.
33 G.J. Tatlock and M. White, J. Appl. Crystallogr., 8 (1975) 49.
34 R.B. Fahim and A.I. Abu-Shady, J. Catal., 71 (1970) 10.
35 R.B. Fahim, M.I. Zaki, R.M. Gabr and S.A.A. Mansour, Surface Technol., 17 (1982) 175.

36 I.F. Hazell and R.J. Irving, J. Chem. Soc. A, (1966) 669.
37 G. Bertrand, M. Lallemant, J.C. Mutin, J.C. Niepce and G. Watelle-Marion, Ann. Chem., 9 (1974) 263.
38 J.C. Niepce, G. Watelle-Marion and C. Clinard, C.R. Acad. Sci. Ser. C, 96 (1972) 274; see also 632 (1969) 269 and 298 (1970) 270.